

Oscillations of a highly discrete breather with a critical regime

E. Coquet, M. Remoissenet, and P. Tchofo Dinda

*Laboratoire de Physique de l'Université de Bourgogne, UMR CNRS No. 5027, Avenue A. Savary,
Boîte Postale 47 870, 21078 Dijon Cédex, France*

(Received 24 January 2000; revised manuscript received 30 June 2000)

We analyze carefully the essential features of the dynamics of a stationary discrete breather in the ultimate degree of energy localization in a nonlinear Klein-Gordon lattice with an on-site double-well potential. We demonstrate the existence of three different regimes of oscillatory motion in the breather dynamics, which are closely related to the motion of the central particle in an effective potential having two nondegenerate wells. In given parameter regions, we observe an *untrapped regime*, in which the central particle executes large-amplitude oscillations from one to the other side of the potential barrier. In other parameter regions, we find the *trapped regime*, in which the central particle oscillates in one of the two wells of the effective potential. Between these two regimes we find a *critical regime* in which the central particle undergoes several *temporary trappings* within an untrapped regime. Importantly, our study reveals that in the presence of purely anharmonic coupling forces, the breather *compactifies*, i.e., the energy becomes abruptly localized within the breather.

PACS number(s): 41.20.Jb, 05.50.+q

I. INTRODUCTION

In recent years there has been considerable effort made in understanding nonlinear energy-localization phenomena [1] in homogeneous discrete lattices. The possibility of existence of localized long-lived molecular vibrational states was pointed out by Ovchinnikov [2] many decades ago. Then, the existence of nonlinear localized modes in a lattice with on-site potential and linear interparticle coupling was explored by Kosevich and Kovalev [3]. Dolgov [4] proposed a model for self-localization of vibrations in a one-dimensional lattice with nonlinear interparticle coupling without on-site potential. Sievers and Takeno [5] reported that large amplitude vibrations in perfectly periodic one-dimensional (1D) lattices can localize because of the nonlinearity and discreteness effects. Then they clearly suggested that *intrinsic localized modes or discrete breathers* should be quite general and robust solutions in the sense that they can exist in many models [5]. This result was subsequently confirmed by Page [6]. In contrast to the case of purely harmonic lattices, where spatially localized modes can occur only when defects or disorder are present so that the translational invariance of the underlying lattice is broken, discrete breathers may be created anywhere in a perfect homogeneous nonlinear lattice. Since the pioneering studies mentioned above [1–6], discrete breathers have been the subject of an intense research (for recent reviews see [7] and [8]), because of their relevance in various fields such as condensed matter physics, optics, and biology. The existence of discrete breathers as exact time periodic spatially localized solutions in a large class of nonlinear lattices was demonstrated analytically by McKay and Aubry [9]. But so far, no analytical derivation of breather solutions in a highly discrete Φ -four lattice has been carried out because of a host of mathematical problems that arise in the specific situation of abrupt localization of energy.

On the other hand, recent studies [10,11] demonstrate that a breathing mode can *compactify* in a nonlinear Klein-Gordon lattice, with a *soft* on-site substrate potential (single-well potential), in the presence of purely anharmonic cou-

pling forces between adjacent particles. The concept of *compactification or strict localization of solitary waves* was introduced for the first time by Rosenau and Hyman [12], who investigated a special type of Korteweg–de Vries equation and discovered that solitary waves can compactify in the presence of a nonlinear dispersion. Such solitary waves, which are characterized by a compact support, i.e., the absence of infinite wings, have been called *compactons*. Then a fundamental question arises as to whether a *breather compacton* can exist in nonlinear Klein-Gordon lattices having an on-site double-well substrate potential. The answer to this question is given in the present paper.

In this paper, we carry out a theoretical analysis showing the existence of a stationary breather in the ultimate degree of energy localization in a nonlinear Klein-Gordon discrete lattice, with a Φ -four on-site substrate potential and very weak coupling forces between adjacent particles. This breather consists of a central particle that executes strongly anharmonic dynamics while all the other particles execute very small-amplitude oscillations about their equilibrium positions. Such a situation, which presents similarities with the localized rotating modes [13], may occur in many discrete real systems where some thermally activated atoms or ions, though coupled to their neighbors, may jump from one site to another one. In the present paper, we provide a general picture describing the oscillatory dynamics of the highly discrete breather, and we show that the on-site double-well potential leads to a much richer spectrum of behavior than there is for the single-well substrate potentials considered in previous studies [10,14]. Most of the richness comes from the existence of several regimes of breather motion, which are closely related to the motion of the central particle of the breather in a double-well effective potential. Many physical processes involving this dynamics may include proton transport in hydrogen-bonded chains [15], planar rotations of base pairs in DNA macromolecules [16], and polymer chains twisting [17].

The paper is organized as follows. In Sec. II we present the model. In Sec. III, we analyze the breather motion in the

untrapped regime, and in Sec. IV we consider the trapped regime. Section V is devoted to the analysis of the critical regime, and in Sec. VI we summarize and give concluding remarks.

II. MODEL

A. Equations of motion

The system under consideration is a nonlinear Klein-Gordon infinite lattice, in which each particle interacts with its nearest neighbors via coupling forces that are either purely harmonic or anharmonic. *Each particle oscillates in a direction perpendicular to the chain axis*, in a Φ -four on-site potential that represents the combined influence of the surrounding lattice atoms and external effects. The lattice Hamiltonian is

$$H = \sum_n \left[\frac{1}{2} \left(\frac{dx_n}{dt} \right)^2 + \frac{c_l}{2} (x_{n+1} - x_n)^2 + \frac{c_{nl}}{4} (x_{n+1} - x_n)^4 + \frac{V_0}{4} (1 - x_n^2)^2 \right]. \quad (1)$$

Here, x_n is the on-site degree of freedom, c_l , c_{nl} , and V_0 are constants that control the strength of linear and nonlinear couplings, and the on-site potential barrier height, respectively. The corresponding one-dimensional equations of motion can be written in the following form:

$$\frac{d^2 x_n}{dt^2} = V_0 [x_n (1 - x_n^2) + C_l (x_{n-1} + x_{n+1} - 2x_n) + C_{nl} [(x_{n-1} - x_n)^3 + (x_{n+1} - x_n)^3]], \quad (2)$$

where $C_l \equiv c_l/V_0$ and $C_{nl} \equiv c_{nl}/V_0$ are the normalized coupling constants.

In the present paper, we examine the *ultimate degree of energy localization* in this nonlinear Klein-Gordon lattice, in the form of a breather. To this end, we consider the *limit of weak coupling between adjacent lattice sites* i.e., a dynamical situation in which only a central particle (CP), say $n = s$, executes a large-amplitude motion from one to the other side of the potential barrier. All the other particles execute relatively small-amplitude oscillations near the bottom of the substrate wells lying in the same side of the potential barrier. Figure 1 shows a schematic representation of the configuration of the system at the beginning of this dynamical situation. The CP is shifted to an unstable position in one side of the substrate potential, labeled ‘‘B’’ in Fig. 1. As a result of the coupling forces, the particles neighboring the CP undergo small shifts, in the same direction as the CP, up to unstable equilibrium positions located near the bottom of the potential wells labeled ‘‘A’’ in Fig. 1. An important point to be emphasized here is that the large initial displacement given to the CP, in the direction perpendicular to the chain axis, generates thereby a symmetry plane (perpendicular to the chain axis), at this lattice site (i.e., s). Consequently, in the limit of no perturbations, the amplitude of displacement of particles $s+i$ and $s-i$ are strictly identical. Thus, at site $n=s$, one can replace Eq. (2) by

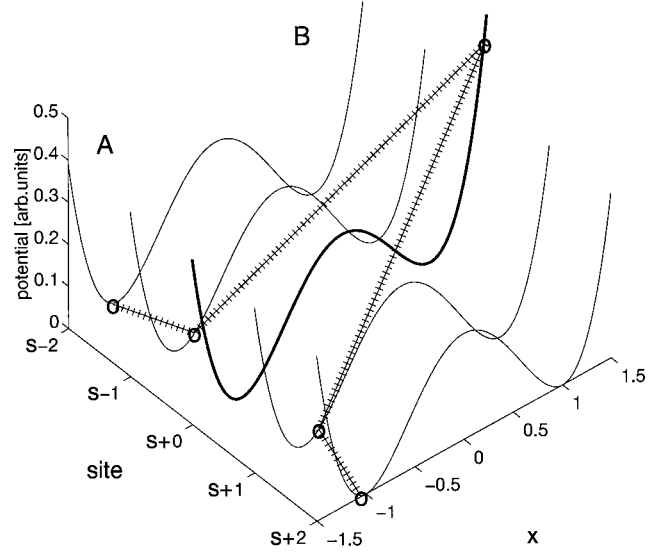


FIG. 1. Schematic representation of the initial configuration of the system in presence of a weak interparticle coupling. The curves represent the on-site substrate potential. The circles represent the particles. The labels ‘‘A’’ and ‘‘B’’ identify the two wells of the potential. The central particle, which lies at the site index ‘‘s,’’ begins its motion in the well B, whereas all the other particles are in the wells A. The particle position x is given in arbitrary units.

$$\frac{d^2 x_s}{dt^2} = V_0 \{ x_s (1 - x_s^2) + 2 [C_l (x_{s\pm 1} - x_s) + C_{nl} (x_{s\pm 1} - x_s)^3] \}. \quad (3)$$

On the other hand, the positions of all the particles, except the CP, can be rewritten as: $x_{s\pm i} = -1 + \Delta x_{s\pm i}$, where the deviation with respect to the equilibrium position is $|\Delta x_{s\pm i}| \ll 1$. Then, for $C_l \ll 1$ and $C_{nl} \ll 1$, the equations of motion at sites s , $s \pm 1$, and $s \pm 2$ reduce, in first-order approximation, to

$$\begin{aligned} \frac{d^2 x_s}{dt^2} &\approx V_0 \{ x_s (1 - x_s^2) - 2 [C_l (1 + x_s) + C_{nl} (1 + x_s)^3] \} \\ &= - \frac{dV_e(x_s)}{dx_s}, \end{aligned} \quad (4)$$

$$\frac{d^2 \Delta x_{s\pm 1}}{dt^2} + 2V_0 \Delta x_{s\pm 1} \approx V_0 [C_l (1 + x_s) + C_{nl} (1 + x_s)^3], \quad (5)$$

$$\frac{d^2 \Delta x_{s\pm 2}}{dt^2} + 2V_0 \Delta x_{s\pm 2} \approx 0. \quad (6)$$

As Eq. (6) shows, in the weak coupling limit, the motion of the $s \pm 2$ particles corresponds essentially to an harmonic oscillation with frequency $\omega_0 = (2V_0)^{1/2}$ and period $T_0 = 2\pi/\omega_0$.

In Eq. (4), V_e represents the effective potential for the CP, whose expression is given by

$$V_e(x) = V_0 \left[\frac{1}{4} (1 - x^2)^2 + C_l (1 + x)^2 + \frac{C_{nl}}{2} (1 + x)^4 \right], \quad (7)$$

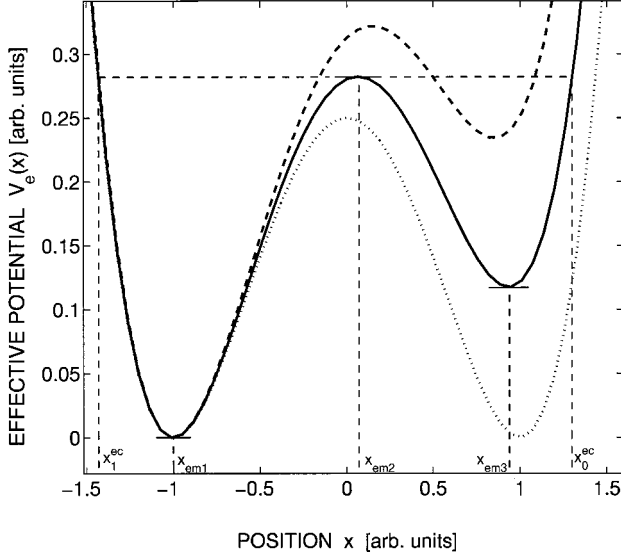


FIG. 2. Schematic representation of the effective potentials for the central particle V_e (solid curve), and for the breather V_{eff} (dashed curve). The dotted curve represent the substrate potential. The parameters x_{em1} , x_{em2} , and x_{em3} , indicate the extrema of the effective potential of the central particle. x_1^{ec} and x_0^{ec} indicate the positions for which $V_e(x) = V_e(x_{em2})$.

with $x \equiv x_s$. Thus, Eqs. (4)–(6) define the motion of the particles that are involved in the breather dynamics in the ultimate degree of energy localization in the system. The effective potential V_e is schematically represented by the solid curve in Fig. 2, where the positions of the extrema of V_e : x_{em1} , x_{em2} , and x_{em3} , can be easily calculated by solving $dV_e(x)/dx = 0$ (the results are given in Table I). One of the effects of the coupling forces is to lower the barrier height of the potential $V_{bh} = V_e(x_{em2}) - V_e(x_{em3})$ that the CP must overcome to move from the well B to the well A . In fact, the ability of the CP to execute a *large-amplitude motion* depends critically on its initial position x_0 . There exists a critical distance x_0^{ec} (from the origin) from which the CP (when released with zero initial velocity) can execute a large-amplitude motion from one to the other side of the potential barrier. Note that in the absence of coupling forces, the effective potential of the CP coincides with the on-site substrate potential represented by the dotted curve in Fig. 2, and there, the critical distance is $x_0^c = \sqrt{2} > x_0^{ec}$. Thus, an outstanding effect of the coupling forces is the reduction of the critical distance from x_0^c to x_0^{ec} (see also Table I). Throughout the present paper, we choose the initial position of the CP to be precisely in the parameter region $x_0 \leq x_0^c$, where the presence of coupling forces is required for the CP to execute an *untrapped motion*. In this region, the breather motion can be broadly divided into three main regimes of oscillatory motion depending on the initial position of the CP.

(i) If $x_0 > x_0^{ec}$, the CP will execute an *untrapped motion* with large-amplitude oscillations.

(ii) When $x_0 < x_0^{ec}$, we find a *trapped regime* in which the potential energy of the CP is not sufficient for this particle to overcome the potential barrier.

(iii) When $x_0 \approx x_0^{ec}$, we find a critical regime in which different situations can occur depending on the precise value

TABLE I. Parameters of the effective potential of the CP $V_e(x)$, for zero, linear and nonlinear coupling cases. The positions of the extrema of $V_e(x)$ are: x_{em1} , x_{em2} , and x_{em3} . V_{bh} is the barrier height. x_0^{ec} is the critical initial position of the CP.

Parameters	No coupling	Linear coupling	Nonlinear Coupling
x_{em1}	-1	-1	-1
x_{em2}	0	$2C_l$	$2C_{nl}$
x_{em3}	1	$1 - 2C_l$	$1 - 8C_{nl}$
V_{bh}	$\frac{V_0}{4}$	$\frac{V_0}{4}(1 - 12C_l)$	$\frac{V_0}{4}(1 - 30C_{nl})$
x_0^{ec}	$\sqrt{2}$	$\sqrt{2}[1 - C_l(1 + \sqrt{2})]$	$\sqrt{2}[1 - C_{nl}(4 + 3\sqrt{2})]$

of x_0 , such as the occurrence of several temporary trappings within an untrapped regime.

We examine successively these three different regimes.

III. UNTRAPPED REGIME

In this regime, the CP has a sufficient energy to overcome the potential barrier. Thus, Eq. (4) can be integrated via a quadrature to give

$$x(w_e t, k_e^2) = x_0 \frac{(p\alpha + \beta) + (\beta - p\alpha)\text{cn}(w_e t, k_e^2)}{(\alpha + \beta) + (\beta - \alpha)\text{cn}(w_e t, k_e^2)}, \quad (8)$$

where the parameters w_e , k_e^2 , p , α , and β , are given in Table II for zero, linear and nonlinear coupling forces, respectively. The function cn in Eq. (8) is a Jacobi elliptic function [18] with modulus $k_e^2 < 1$. Solution (8) corresponds to oscillations of period T_e and frequency Ω :

$$T_e = \frac{4}{w_e} K(k_e^2) \quad \text{with} \quad K(k_e^2) = \int_0^{\pi/2} \frac{du}{\sqrt{1 - k_e^2 \sin^2 u}} \quad \text{and} \quad \Omega = \frac{2\pi}{T_e}. \quad (9)$$

For very weak coupling: $C_l \ll 1$ and $C_{nl} \ll 1$ (including the case when $C_l = C_{nl} = 0$), the general solution (8) can be approximated [18] by

$$x(t) \approx x_0 \text{cn}(w_e t, k_e) \approx x_0 \sum_{n=0}^{\infty} P_{2n+1} \cos(2n+1)\Omega t, \quad (10)$$

where

$$P_{2n+1} = \frac{\pi}{k_e K(k_e^2)} \cosh^{-1} \left(\pi \left(n + \frac{1}{2} \right) \frac{K(1 - k_e^2)}{K(k_e^2)} \right). \quad (11)$$

Solution (10) shows that the central-particle motion, which is closely related to the breather motion, is made up of the fundamental frequency Ω and several odd harmonics. This behavior is formally equivalent to large-amplitude oscillations of a particle in a double-well potential [19,20]. The substitution of the expressions for w_e and k_e (see Table II) in Eq. (9) gives the period T_e in terms of the initial condition x_0

TABLE II. Characteristic parameters w_e , k_e^2 , p , α^2 , and β^2 , for the CP motion in the untrapped regime, for zero $(C_l, C_{nl}) = (0, 0)$, linear $(C_l, 0)$ and nonlinear $(0, C_{nl})$ coupling.

(C_l, C_{nl})	$w_{e(C_l, C_{nl})}$
(0,0)	$V_0(x_0^2 - 1)$
$(C_l, 0)$	$w_{e(0,0)} \left[1 + \frac{C_l}{(x_0^2 - 1)^2} (x_0^2 + 2x_0 - 1) \right]$
$(0, C_{nl})$	$w_{e(0,0)} \left(1 + \frac{C_{nl}}{(x_0^2 - 1)^2} [x_0^4 + 2(x_0^3 + x_0^2 + x_0) - 3] \right)$
(C_l, C_{nl})	$k_{e(C_l, C_{nl})}^2$
(0,0)	$\frac{x_0^2}{2(x_0^2 - 1)}$
$(C_l, 0)$	$k_{e(0,0)}^2 \left[1 - \frac{2C_l}{x_0(x_0^2 - 1)^2} (x_0^3 - x_0 + 2) \right]$
$(0, C_{nl})$	$k_{e(0,0)}^2 \left[1 - \frac{4C_{nl}}{x_0(x_0^2 - 1)^2} (2x_0^3 + x_0^2 - 2x_0 + 1) \right]$
(C_l, C_{nl})	$p_{(C_l, C_{nl})}$
(0,0)	-1
$(C_l, 0)$	$-\left(1 + \frac{4C_l}{x_0(x_0^2 - 1)} \right)$
$(0, C_{nl})$	$-\left(1 + \frac{4C_{nl}(1 + x_0^2)}{x_0(x_0^2 - 1)} \right)$
(C_l, C_{nl})	$\alpha_{(C_l, C_{nl})}^2$
(0,0)	$2(x_0^2 - 1)$
$(C_l, 0)$	$2(x_0^2 - 1) + 4C_l$
$(0, C_{nl})$	$2(x_0^2 - 1) + 8C_{nl}(2 + x_0)$
(C_l, C_{nl})	$\beta_{(C_l, C_{nl})}^2$
(0,0)	$2(x_0^2 - 1)$
$(C_l, 0)$	$2(x_0^2 - 1) + 4C_l \left(1 + \frac{4x_0}{x_0^2 - 1} \right)$
$(0, C_{nl})$	$2(x_0^2 - 1) + 8C_{nl} \left(2 + \frac{x_0(x_0^2 + 3)}{x_0^2 - 1} \right)$

and the coupling parameters. The dotted-dashed curve in Fig. 3 represents the normalized period T_e/T_0 for oscillations of the CP as a function of its initial position x_0 , in the absence of coupling. T_e/T_0 becomes infinite when the initial position of the CP coincides with the critical value: $x_0 = x_0^c = \sqrt{2}$ (as indicated in Fig. 3 by a vertical dotted line). Thus, in the absence of coupling, the CP would be unable to cross the potential barrier for initial positions such that $x_0 \leq x_0^c$. In the presence of coupling, T_e is represented by the solid curves in Fig. 3, which show that the CP is now able to cross the potential barrier for initial positions below x_0^c , in the region $x_0^{ec} \leq x_0 \leq x_0^c$. Here, the coupling plays a crucial role in the sense that it is required for the CP to execute large-amplitude oscillations from one to the other side of the potential barrier. On the other hand, the achievement of the ultimate degree of

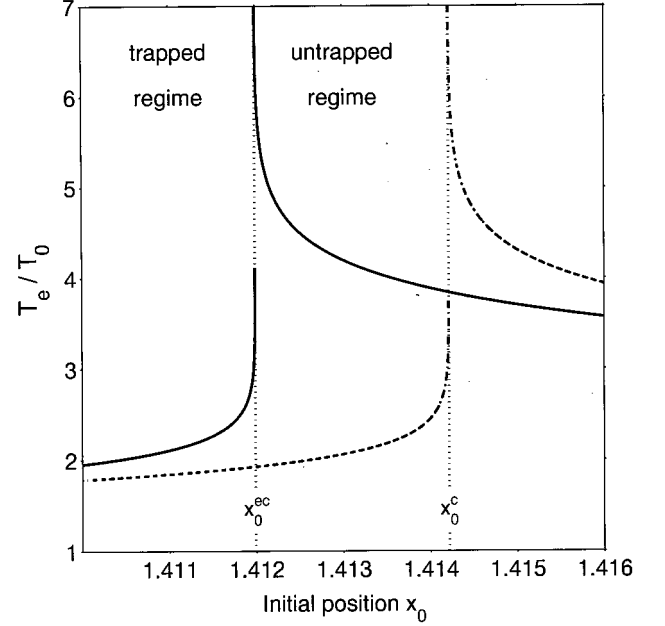


FIG. 3. Plot showing the normalized period of oscillations T_e/T_0 in the effective potential V_e , as a function of the initial position of the central particle x_0 , for $C_l = 6.5 \times 10^{-4}$ and $C_{nl} = 0$ (solid curves), T_0 being the period of small-amplitude oscillations in the bottom of one of the two degenerate wells of the substrate potential. The dotted-dashed curves represent the period of oscillations in the on-site substrate potential ($C_l = 0$ and $C_{nl} = 0$).

energy localization in the breather imposes a strict limitation in the strength of linear or nonlinear coupling, to ensure small-amplitude oscillations for all the particles other than the CP. As a consequence, the size of the parameter region $x_0^{ec} \leq x_0 \leq x_0^c$ must be sufficiently small. Hereafter, we use $C_l = 6.500 \times 10^{-4}$ and $C_{nl} = 1.909 \times 10^{-4}$, for which $x_0^{ec} = 1.41199$.

Although the CP plays the prominent role in the motion of a highly localized breather mode, the role of the other particles of the system cannot be ignored in a discrete system, because they are involved in the energy-exchange or compactification processes, which we discuss below. An analytical description of the motion of these particles ($s \pm 1$) may be obtained by rewriting Eq. (5) as follows:

$$\frac{d^2 \Delta x_{s \pm 1}}{dt^2} \approx -\omega_0^2 \Delta x_{s \pm 1} + V_0 G(t), \quad (12)$$

where the function G in the right-hand side of Eq. (12) is given by

$$\begin{aligned} G(t) &= G_l(t) + G_{nl}(t) \\ &= C_l [1 + x(t)] + C_{nl} [1 + x(t)]^3 \\ &= C_l \left[1 + x_0 \sum_{n=0}^q P_{2n+1} \cos(2n+1)\Omega t \right] \\ &\quad + C_{nl} \left[1 + x_0 \sum_{n=0}^q P_{2n+1} \cos(2n+1)\Omega t \right]^3, \quad (13) \end{aligned}$$

TABLE III. Characteristic parameters g_{iQ} for linear $Q=l$ and nonlinear $Q=nl$ coupling, for the motion of particles $s \pm 1$ in the untrapped regime, described by Eqs. (14), (15), and (16).

Linear coupling (g_{il})	Nonlinear coupling (g_{inl})
$g_{0l} = C_l$	$g_{0nl} = C_{nl} \left(1 + \frac{3x_0^2}{2} (P_1^2 + P_3^2) \right)$
$g_{1l} = C_l x_0 P_1$	$g_{1nl} = 3C_{nl} x_0 P_1 \left[1 + \frac{x_0^2}{4} (P_1^2 + P_1 P_3 + 2P_3^2) \right]$
$g_{2l} = 0$	$g_{2nl} = C_{nl} \frac{3x_0^2}{2} (P_1^2 + 2P_1 P_3)$
$g_{3l} = C_l x_0 P_3$	$g_{3nl} = C_{nl} \left[\frac{(x_0 P_1)^3}{4} + 3x_0 P_3 \left(1 + \frac{x_0^2}{4} (P_3^2 + 2P_1^2) \right) \right]$
$g_{4l} = 0$	$g_{4nl} = 3C_{nl} x_0^2 P_1 P_3$

q is an integer whose value depends on the order of approximation that is desired. The functions $G_l(t)$ and $G_{nl}(t)$ can be rewritten into the general form

$$G_Q(t) = \sum_{i=0}^J g_{iQ} \cos(i\Omega t), \quad (14)$$

where the index Q stands for l or nl . The coefficients g_{iQ} are given in Table III for the highest-amplitude harmonics ($i = 0, 1, 2, 3, 4$). Keeping only these harmonics, with the initial conditions: $\Delta x_{s \pm 1}(0) \approx 0$, and $\Delta \dot{x}_{s \pm 1}(0) \approx 0$, we obtain the following *approximate* solution for Eq. (12):

$$\Delta x_{s \pm 1}(t) \approx \sum_{n=0}^J X_n \sin \left[\left(1 + \frac{n}{m} \right) \frac{\omega_0 t}{2} \right] \sin \left(\frac{\Delta \omega_n t}{2} \right), \quad (15)$$

where we have set

$$m = \frac{\omega_0}{\Omega}, \quad \Delta \omega_n = \left(1 - \frac{n}{m} \right) \omega_0, \quad X_n = \frac{m^2}{m^2 - n^2} g_{nQ}. \quad (16)$$

Equation (15) shows that the motion of the particles ($s \pm 1$) depends strongly on the coupling parameters (C_l, C_{nl}) through X_n , which depends on g_{nQ} . Furthermore, the amplitudes X_n in Eq. (15) become infinite when $m = \omega_0 / \Omega$ is a nonzero integer. This resonant process is only qualitatively correct because of the approximate nature of Eq. (15). A resonant phenomenon can thus occur in the system if a higher-order harmonic of the breather coincides with the frequency of small-amplitude oscillations (in the bottom of one of the two wells of the substrate potential), ω_0 . All of the above qualitative considerations are remarkably well-confirmed by the numerical simulations that we have performed using the equations of motion of the system, Eq. (2). The numerical method used to obtain the initial configuration of the breather, as schematically represented in Fig. 1, is the so-called ‘‘relaxation process’’ [21]. We accomplish this relaxation by, first, putting the CP to a given position x_0 (in the potential well labeled ‘‘B’’ in Fig. 1), and all the other particles in the bottom of the wells ‘‘A.’’ Then, we let all the particles (except the CP) to move according to Eq. (2). Peri-

odically, the velocities of all those particles are set to zero after a specified number of time steps. In doing so, we periodically extract energy from the system until all the particles cease to move. Once this process is completed, the effective potential V_{eff} of the breather can be obtained from the following expression (taking into account all particles of the chain):

$$V_{\text{eff}} \equiv \sum_n V_0 \left[\frac{C_l}{2} (x_{n+1} - x_n)^2 + \frac{C_{nl}}{4} (x_{n+1} - x_n)^4 + \frac{1}{4} (1 - x_n^2)^2 \right], \quad (17)$$

which is schematically represented by the dashed curve in Figs. 2, in a very qualitative way. Indeed, this potential differs clearly from the effective potential V_e of the CP (solid curve in Fig. 2) only when the strength of the coupling forces is sufficiently important. In the weak coupling limit under consideration throughout the present paper, V_{eff} is essentially identical to V_e . Hereafter, unless otherwise specified, we take $V_0 = 1$.

A. Linear coupling

Figures 4, that we have obtained for $x_0 = 1.414$, show that as soon as the CP is released from a position $x_0 > x_0^{ec} = 1.41199$, it executes a large-amplitude oscillatory motion from one to the other side of the potential barrier [see Fig. 4(a1)]. In Figs. 4(a1), 4(b1), 4(c1), and 4(d1), we have represented the motion of the CP (s) and its neighbors: $s \pm 1$, $s \pm 2$, $s \pm 3$, and in Figs. 4(a2), 4(b2), 4(c2), and 4(d2), the Fourier spectra of each motion, respectively. These spectra reveal that the breather motion is made up of a fundamental frequency Ω and a few higher-order harmonics $n\Omega$. But, only odd harmonics contribute to the breather motion and those harmonics are present in the motion of all the particles that make up the breather, i.e., the CP and its nearest neighbors $s \pm 1$. Furthermore, we see that particles $s \pm 2$ and $s \pm 3$ oscillate at the phonon frequency ω_0 with amplitudes that increase in time (at least in the first stage of the dynamics). This behavior indicates that a small amount of the energy that was initially localized on the three particles, s and $s \pm 1$, is progressively transferred to other lattice sites through a phonon-radiation process. Indeed, owing to the linear coupling, a phonon band: $\omega_k = \omega_0 [1 + 2C_l \sin^2 k/2]^{1/2}$, $0 \leq k \leq \pi$, exists in the frequency spectrum of the system, whether the breather is present or not in the lattice. In the very weak coupling limit that we consider, the upper phonon band edge lies very close to ω_0 . Thus, the breather motion acts as a source of excitation of the phonon spectrum, leading to small oscillations at frequency ω_0 for particles that lie away from the breather, as Figs. 4(c2) and 4(d2) show. The conversion of the CP energy into phonon-mode energy occurs in a relatively smooth and continuous manner (low-conversion regime).

As mentioned above, the breather motion involves a fundamental frequency Ω that always lies in the gap below the lower-phonon band edge: $\Omega < \omega_0$. Consequently, as Ω depends on the initial position x_0 of the CP (see Fig. 3), a higher-order harmonic of Ω may (for some specific values of

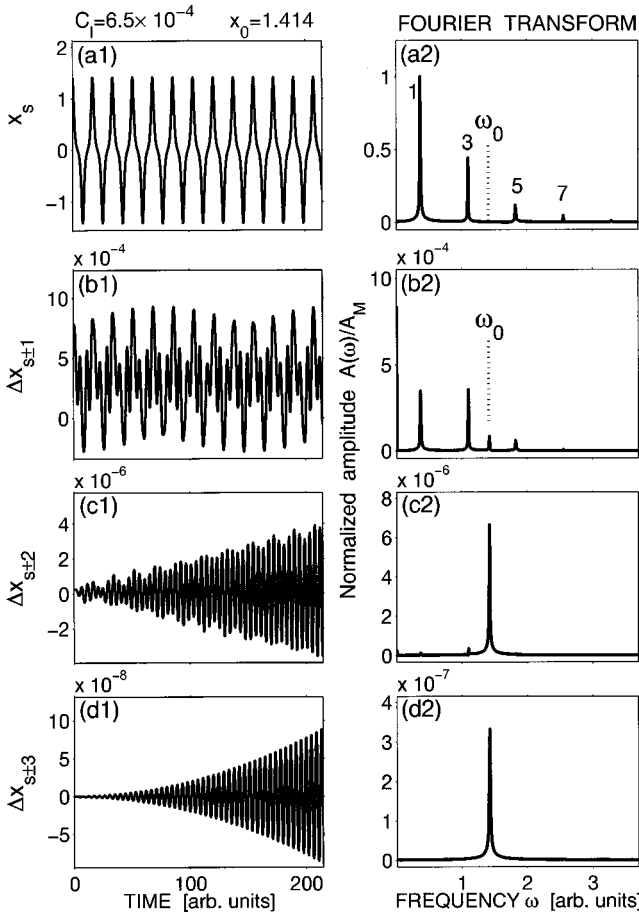


FIG. 4. Plots showing the temporal evolution of the positions (in arb. units) of particles that make up the breather motion, obtained by solving exactly the discrete equations of motion (2), for $x_0 = 1.414$, $C_l = 6.5 \times 10^{-4}$ and $C_{nl} = 0$. (a1): $x_s(t)$. (b1): $\Delta x_{s\pm 1}(t) = 1 + x_{s\pm 1}(t)$. (c1): $\Delta x_{s\pm 2}(t) = 1 + x_{s\pm 2}(t)$. (d1): $\Delta x_{s\pm 3}(t) = 1 + x_{s\pm 3}(t)$. t designates the time (in arb. units). (a2), (b2), (c2), and (d2) show the Fourier transforms of the motion represented in (a1), (b1), (c1), and (d1), respectively. Each peak in (a2) and (b2) corresponds to an harmonic $n\Omega$ of the breather motion. In (a2), the labels ‘‘1,’’ ‘‘3,’’ ‘‘5,’’ and ‘‘7’’ indicate the harmonics that are present in the CP motion.

x_0) make direct resonance with phonon modes, thus producing a strong transfer of energy away from the breather (strong-conversion regime). Such a situation is represented in Figs. 5, where for $x_0 = 1.4122$ we have represented the motions of the CP and particles $s \pm 1$ and their respective Fourier spectra. Note that the size of the phonon band is so small that only a single harmonic can be present inside this phonon band $\omega_0 \leq n\Omega \leq \omega_\pi = [\omega_0^2 + 4C_l]^{1/2}$. The resonance phenomenon observed in Fig. 5(a2) results from the presence of the harmonic $n=5$ in the phonon band, which causes a large enhancement of the amplitude of oscillations for all particles (except the CP), in particular for particles that are far away from the CP. For example, in the strong-conversion regime, the amplitude of oscillations for the particles $s \pm 2$ and $s \pm 3$ is by more than one order of magnitude larger than in the low-conversion regime [compare Fig. 4(c1) with Fig. 5(c1), or Fig. 4(d1) with Fig. 5(d1)]. However, it is worth noting in Fig. 5(a1) that this strong conversion regime does not cause a substantial drop in the amplitude of the CP os-

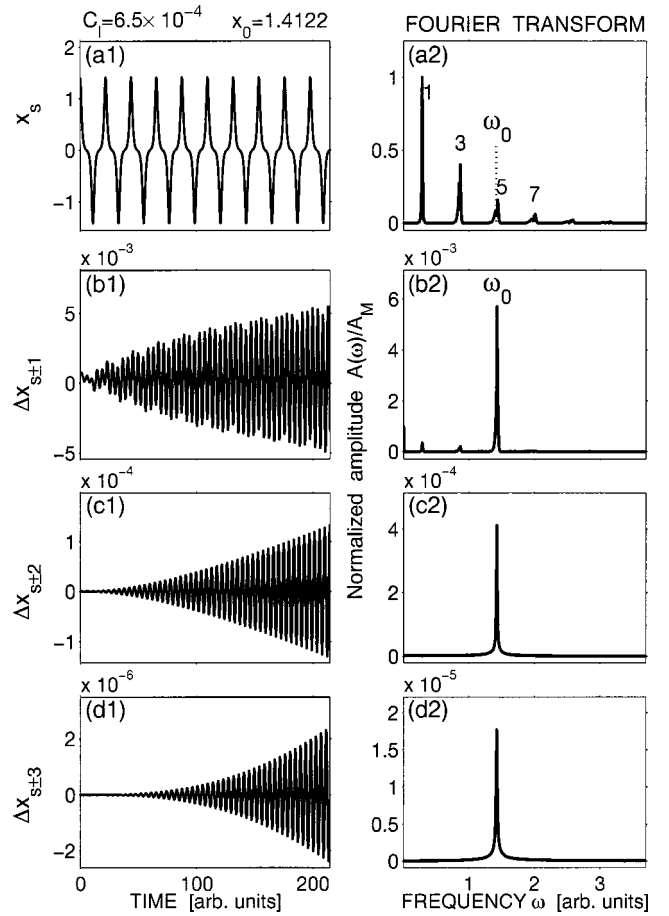


FIG. 5. Plots obtained in the same conditions as for Figs. 4, but with $x_0 = 1.4122$.

cillations, owing to the weakness of the coupling forces between adjacent particles.

B. Nonlinear coupling

For $x_0 = 1.414$, $C_l = 0$, and $C_{nl} = 1.909 \times 10^{-4}$, Figs. 6(a1) and 6(a2) show that, the CP motion exhibits the same general features as for the linear coupling cases considered above [Figs. 4(a1) and 4(a2), and Figs. 5(a1) and 5(a2)] in the sense that only odd harmonics of the breather motion are present in the CP motion. Figs. 6(b1) and 6(b2) reveal the presence of all harmonics (odd and even) in the motion of the nearest neighbors of the CP, whereas only odd harmonics are present in the linear coupling case [see Figs. 4(b1) and 4(b2), and Figs. 5(b1) and 5(b2)]. Moreover, we see in Figs. 6(a1), 6(b1), and 6(c1) that the amplitude of oscillations of particles lying away from the CP decreases abruptly from $x_s > 1$ (for the CP) to $\Delta x_{s\pm 2} \sim 10^{-10}$, and no appreciable motion is detected for particles $s \pm 3$. *This abrupt localization of energy within the breather demonstrates the ability of a breather to ‘‘compactify’’ in a nonlinear Klein-Gordon lattice with an on-site double-well potential.* However, we are unable to prove analytically that we have a ‘‘compactonic’’ behavior in a strict mathematical sense. *Nevertheless, such breathers will be referred to as compactons in a physical sense (i.e., a discrete breather with abrupt localization).* In this context, the energy localization on only three particles ($s, s \pm 1$) corresponds to the ultimate degree of energy localization in a

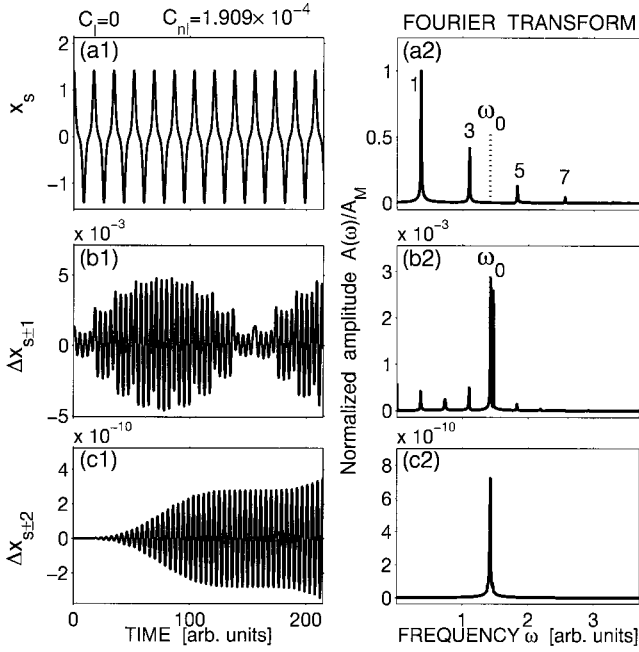


FIG. 6. Plots showing the evolution of the positions (in arb. units) of particles that make up the breather motion, for $x_0 = 1.414$, $C_l = 0$, and $C_{nl} = 1.909 \times 10^{-4}$. (a1): $x_s(t)$. (b1): $\Delta x_{s \pm 1}(t)$ (c1): $\Delta x_{s \pm 2}(t)$. t designates the time (in arb. units). (a2), (b2), and (c2) show the Fourier transforms of the motion represented in (a1), (b1), and (c1), respectively.

discrete breather. Furthermore, Fig. 6(b2) shows that the chosen initial particle position $x_0 = 1.414$ corresponds to a situation where the fourth harmonic of the breather motion resonates with phonon modes. As a result, the amplitudes of oscillations of particles $s \pm 2$ [see Fig. 6(c1)] are found to be, by more than one order of magnitude, larger than the corresponding amplitudes in any off-resonant case in the region $x_0 \approx 1.414$. Thus, the compactification of the breather is preserved even in the presence of the resonance phenomenon, as long as the coupling forces are sufficiently weak.

As a general remark for the whole untrapped regime, it is worth noting that the deviation between the analytical expression of the CP motion in Eq. (8), $x(t)$, and the numerical solutions $X_s(t)$, measured by $\Lambda = \sum_n [X_s(n dt) - x(n dt)]^2 / x_0$ (where dt is the time step) does not exceed 2%. Equation (8) therefore provides a highly accurate representation of the CP motion in the untrapped regime.

IV. TRAPPED REGIME

In this regime, the CP starts out at a position $x_0 < x_0^{ec}$, with a potential energy that is below the critical level for crossing the barrier of the effective potential: $V_e(x_0) < V_e(x_{em2})$ (see Fig. 2). The CP is therefore trapped in the shallower well while all the other particles oscillate in the deepest well. This situation, which has been largely neglected in all previous discretized field theories of a breather motion, makes one of the greatest qualitative differences with respect to the breather motion in a lattice with a single-well on-site potential (in which only a single regime exists) [10]. In the weak coupling limit, Eq. (4) can be integrated via a quadrature, in a similar way as for the untrapped regime in

TABLE IV. Characteristic parameters \hat{k}_e^2 for the CP motion in the trapped regime, for zero (0,0), linear ($C_l, 0$) and nonlinear ($0, C_{nl}$) coupling.

(C_l, C_{nl})	$\hat{k}_{e(C_l, C_{nl})}^2$
(0,0)	$\frac{2(x_0^2 - 1)}{x_0^2}$
$(C_l, 0)$	$\hat{k}_{e(0,0)}^2 \left[1 + \frac{2C_l(x_0^2 - 1 + x_0 - 2(2 - x_0^2)^{1/2})}{(x_0^2 - 1)^2} \right]$
$(0, C_{nl})$	$\hat{k}_{e(0,0)}^2 \left[1 + \frac{2C_{nl}(x_0^3 + x_0 + 4(x_0^2 - 1) + (x_0^2 - 3)(2 - x_0^2)^{1/2})}{(x_0^2 - 1)^2} \right]$

Sec. III. The solution, in terms of the Jacobi elliptic function dn [18] with modulus $\hat{k}_e^2 < 1$, may be written as

$$x(t) \approx x_0 \text{dn}(\hat{w}_e t, \hat{k}_e^2), \quad (18)$$

where $\hat{w}_e(C_l, C_{nl}) \approx \hat{w}_e(0,0) = x_0(V_0/2)^{1/2}$. The parameters $\hat{k}_e^2(C_l, C_{nl})$ are displayed in Table IV. Solution (18) corresponds to oscillations of period \hat{T}_e and frequency $\hat{\Omega}$:

$$\hat{T}_e = \frac{2}{\hat{w}_e} K(\hat{k}_e^2) \quad \text{with} \quad K(\hat{k}_e^2) = \int_0^{\pi/2} \frac{du}{\sqrt{1 - \hat{k}_e^2 \sin^2 u}} \quad \text{and} \quad \hat{\Omega} = \frac{2\pi}{\hat{T}_e}. \quad (19)$$

In the weak coupling limit, Eq. (18) can be rewritten as (see Ref. [18]):

$$x(t) \approx x_0 \left[\frac{\pi}{2K(\hat{k}_e^2)} + \sum_{n=1}^{\infty} Q_{2n} \cos(2n\hat{\Omega}t) \right], \quad \hat{\Omega} = 2\pi/\hat{T}_e, \quad (20)$$

where

$$Q_{2n} = \frac{\pi}{K(\hat{k}_e^2)} \cosh^{-1} \left(\pi n \frac{F(1 - \hat{k}_e^2)}{K(\hat{k}_e^2)} \right). \quad (21)$$

On the other hand, we have found from numerical simulations that in the trapped regime the breather exhibits the same general features in both linear and nonlinear coupling cases, except that in the nonlinear case the breather energy is abruptly localized on the CP and its nearest and next-nearest neighbors. We present below only this latter case.

Figures 7, which show the numerical solution of Eqs. (2) for $x_0 = 1.410$, represent a typical breather motion. Figure 7(a1) shows that the CP moves off the initial position x_0 (in the shallower well) and attempts to proceed to the deepest well of the effective potential, but cannot do so because its kinetic energy is not sufficient to overcome the potential barrier. As a result, the CP remains trapped in this shallow well during the ensuing motion, with an amplitude of oscillations

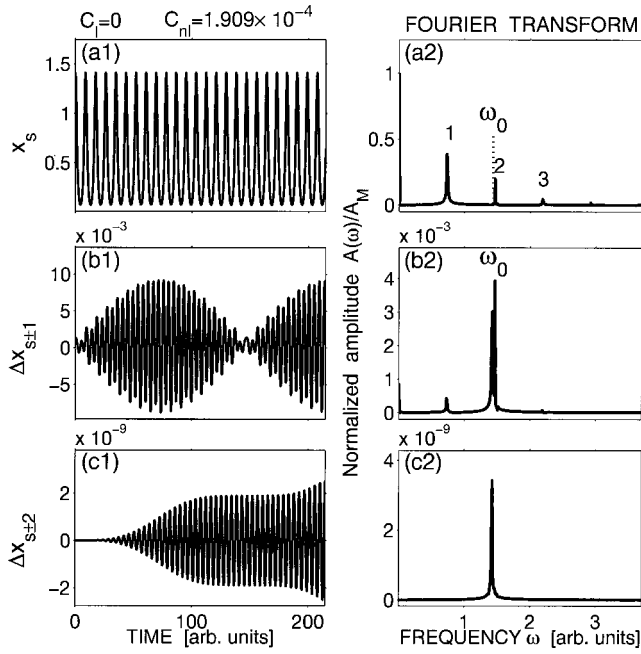


FIG. 7. Plots showing the particle dynamics in the trapped regime of the CP, for $x_0 = 1.410$, $C_l = 0$ and $C_{nl} = 1.909 \times 10^{-4}$.

that is nearly half of the amplitude for a typical untrapped regime. Moreover, the mean positions of the particles are shifted in the direction of the shallow well, thus leading to the presence of a dc component in the Fourier transform of the motion of those particles [see Figs. 7(a2) and 7(b2)]. Even and odd harmonics are present in the motion contrary to the untrapped regime with linear coupling forces, where only odd harmonics are present in the breather motion [Figs. 4(a2) and 4(b2), or Figs. 5(a2) and 5(b2)]. Furthermore, Figs. 7(a2) and 7(b2) demonstrate that the chosen initial condition for the CP corresponds to a situation where a resonance occurs, owing to the presence of the second harmonic in the phonon band. The amplitude of oscillation for particles $s \pm 2$ remains within $\approx 10^{-9}$, and no appreciable motion was detected for the other particles. This behavior therefore reveals the ability of a Φ -four breather to *compactify* in the trapped regime.

As a general remark, for all the trapped regimes, we note that the deviation between the CP motion in Eq. (18), and the numerical solutions, measured by Λ (defined above), does not exceed 5%; which corresponds to a fairly good agreement.

V. CRITICAL REGIME

When the CP is released from position $x_0 \approx x_0^{ec}$, its energy is just sufficient to overcome the potential barrier. In this case, the breather motion depends critically on the energy transfer process from the CP to the neighboring lattice sites. The dynamics can be arbitrarily divided into two main categories of breather oscillations, which are discussed below for the linear coupling case only, because the dynamical behavior in the nonlinear coupling case is similar.

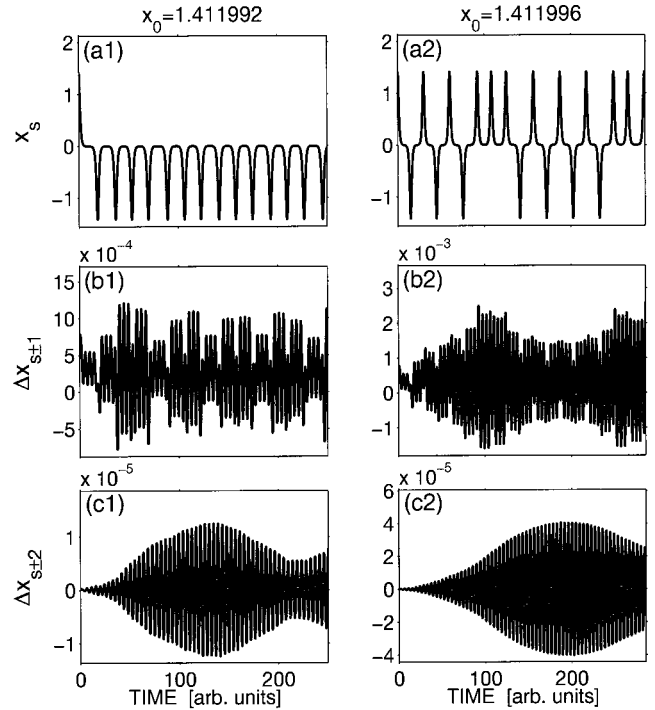


FIG. 8. Plots showing the particle dynamics in the critical regime for $C_l = 6.5 \times 10^{-4}$ and $C_{nl} = 0$. $x_0 = 1.411992$: (a1), (b1), and (c1). $x_0 = 1.411996$: (a2), (b2), and (c2).

A. Trapped regime in the deepest well of the effective potential

In the presence of linear coupling forces, for $x_0 = 1.411992$, Fig. 8(a1) shows a particular situation in which the CP is initially untrapped and then becomes trapped in the deepest well. The CP potential energy is initially sufficient to permit it to overcome the potential barrier. The CP moves up to the deepest well of the effective potential, reaches the turning point, then begins to travel back to the shallow well, and finally has an energy that is no longer sufficient for crossing the potential barrier. It is therefore trapped in the deepest well of the potential during the ensuing oscillatory motion. We attribute this trapping to the fact that, a small fraction of CP energy is converted into energy for its neighbors, through a phonon emission process, as we already mentioned above. Although this energy conversion process is very weak in case of small coupling forces, it is sufficient to play a crucial role in the critical regime.

B. Temporary trapping

When the initial position is $x_0 = 1.411996$ [slightly larger than x_0 in Fig. 8(a1)] the energy is just sufficient for the CP to execute several untrapped oscillations in the beginning of its motion. In this case, Fig. 8(a2) shows that the CP executes several untrapped oscillations at one go, before undergoing a transition to the trapped regime. A careful examination of Fig. 8 (b2) reveals that the trapping of the CP occurs precisely when the amplitude of oscillations of the nearest neighbors, $s \pm 1$, attains its maximum (at $t \approx 100$). In other words, this trapping occurs exactly when a part of energy that was initially stored in the CP is transferred to the nearest neighbors $s \pm 1$ (amplitude $\approx 2 \times 10^{-3}$). Then, after a while, the energy lost by the CP is (at least in part) transferred back

to the CP while this particle is moving in the direction of the potential barrier; which permits the CP to cross again the potential barrier. So, the CP executes several untrapped oscillations, until a second *temporary trapping* occurs. We observe in Fig. 8(a2) that the CP undergoes several *temporary trappings* in this untrapped regime. Thus, the existence of a critical regime for a Klein-Gordon breather makes the greatest qualitative difference with previous studies on the breather dynamics in nonlinear Klein-Gordon systems. Our results in Figs. 8 therefore demonstrate that Klein-Gordon breathers are collective entities that possess a much richer temporal structure of modes than that of a simple particle.

VI. CONCLUSION

We have investigated theoretically the dynamics of a highly discrete breather in the ultimate degree of energy localization in a nonlinear Klein-Gordon lattice, with weak interparticle coupling, submitted to a Φ -four substrate potential. In this system, the central particle (CP) executes relatively large-amplitude nonlinear oscillations, while all the other particles of the lattice execute small-amplitude oscillations around their equilibrium positions. For this Φ -four breather, we have demonstrated the existence of several regimes of oscillatory motion.

(i) We have observed an untrapped regime in which the CP executes large-amplitude oscillations from one to the other side of the potential barrier.

(ii) In other parameter regions, we find the *trapped regime*, in which the CP is trapped in one of the two wells of its effective potential throughout its motion. Since the coupling forces breaks the symmetry of the two wells of the effective potential of the CP, two types of trapped regimes can occur depending on whether this CP is trapped in the deepest or shallower well of the potential. The trapped regime in the deepest well corresponds to the case where all the particles that make up the breather oscillate on the same side of the potential barrier, whereas the trapped regime in the well with the smallest depth corresponds to the case where the CP oscillates in the shallow well while all the other particles oscillate in the deepest well.

(iii) Between the *untrapped* and *trapped* regimes, we have identified a *critical regime*, which occurs when the CP starts out its motion in the shallower well with an energy that is just sufficient to cross the potential barrier. Then the CP undergoes several *temporary trappings* within an *untrapped regime*. This temporary trapping occurs because energy is transferred from the CP to the nearest neighbors. However, the nearest neighbors can synchronously transfer energy back to the CP precisely when this particle is attempting to cross the potential barrier, which then causes the CP to be-

come untrapped. This behavior result makes the greatest qualitative difference from previous work [10] and related studies on breather dynamics [14,22].

On the other hand, we have shown that although the coupling forces between adjacent particles are very weak, in all the regimes mentioned above, a very small fraction of the breather energy is lost through a phonon-radiation process. In general, this energy-radiation process occurs in a continuous and smooth manner, in the form of phonons that are emitted around the fundamental frequency ω_0 with a nearly zero group velocity. Consequently, those phonons do not propagate far away from the breather, thus preserving a high degree of energy localization within the breather. However, we have found some particular conditions for which the energy-transfer process is much stronger than in the case mentioned above. The mechanism of this strong emission of phonons involves a parametric coupling between phonon modes and the harmonics of a fundamental frequency Ω associated with the breather motion. A strong phonon emission occurs whenever the initial position of the CP is such that a higher-order harmonic of the breather motion, $n\Omega$, falls in the phonon band. In the situation of high degree of energy localization, almost all the energy of the breather is located on the CP at least in the beginning of the motion. Then, the phonon emission process induces a small transfer of energy from the CP to particles lying away from the breather. A *major result of the present paper is the demonstration that in case of purely anharmonic coupling forces between adjacent particles, the amplitude of oscillations of the particles neighboring the CP decreases to zero beyond the next-nearest neighbors. This behavior in a nonlinear Klein-Gordon lattice with an on-site double-well potential reveals the ability of a breather to compactify.*

In this context, the concept of compactification of solitary waves [10,12,14,22,23] suggests the possibility of existence of collective entities with a strict localization of energy in physical nonlinear systems such as hydrogen-bonded chains, DNA macromolecules, or polymer chains, as mentioned in the Introduction. This concept should be especially interesting for systems such as fiber transmission links in communications systems, in which solitary waves with compact support would have as a main advantage compared to classical solitons, the absence of long-range interaction between adjacent waves. From a fundamental point of view, an understanding of the behavior of structures with a high degree of energy localization in simple nonlinear systems constitutes a useful step toward the generic physical mechanisms that govern the generation and stability of localized nonlinear waves. In more complicated systems, these processes may involve strongly anharmonic local dynamics of one atom or ion.

[1] A. C. Scott and L. Macneil, Phys. Lett. A **98**, 87 (1983).
 [2] A. A. Ovchinnikov, Zh. Eksp. Teor. Fiz. **57**, 263 (1969) [Sov. Phys. JETP **30**, 147 (1970)].
 [3] M. A. Kosevich and A. S. Kovalev, Zh. Eksp. Teor. Fiz. **67**, 1793 (1974) [Sov. Phys. JETP **40**, 891 (1974)].
 [4] A. S. Dolgov, Fiz. Tverd. Tera (Leningrad) **28**, 1641 (1986) [Sov. Phys. Solid State **28**, 907 (1986)].

[5] A. J. Sievers and S. Takeno, Phys. Rev. Lett. **61**, 970 (1988).
 [6] J. B. Page, Phys. Rev. B **41**, 7835 (1990).
 [7] S. Aubry, Physica D **103**, 201 (1997).
 [8] S. Flach and C. R. Willis, Phys. Rep. **295**, 181 (1998).
 [9] R. S. MacKay and S. Aubry, Nonlinearity **7**, 1623 (1994).
 [10] P. Tchofo Dinda and M. Remoissenet, Phys. Rev. E **60**, 6218 (1999).

- [11] M. Remoissenet, *Waves Called Solitons Concepts and Experiments*, 3rd ed. (Springer-Verlag, Berlin, 1999).
- [12] P. Rosenau and J. M. Hyman, *Phys. Rev. Lett.* **70**, 564 (1993).
- [13] S. Takeno and M. Peyrard, *Phys. Rev. E* **55**, 1922 (1997); D. Bonart and J. B. Page, *Phys. Rev. E* **60**, R1134 (1999).
- [14] Yuri S. Kivshar, *Phys. Rev. E* **48**, 43 (1993).
- [15] O. M. Braun, F. Zhang, Y. S. Kivshar, and L. Vasquez, *Phys. Lett. A* **157**, 241 (1991).
- [16] S. Takeno and S. Hamma, *J. Phys. Soc. Jpn.* **55**, 65 (1986).
- [17] F. Fillaux and C. J. Carlile, *Phys. Rev. B* **42**, 5990 (1990).
- [18] P. F. Byrd, *Handbook of Elliptic Integrals for Engineers and Physicists* (Springer-Verlag, Berlin, 1971).
- [19] Y. Onodera, *Prog. Theor. Phys.* **44**, 1477 (1970).
- [20] M. Iwamatsu and Y. Onodera, *Prog. Theor. Phys.* **57**, 699 (1977).
- [21] R. Boesch, C. R. Willis, and M. El-Batanouny, *Phys. Rev. B* **40**, 2284 (1989).
- [22] S. Dusuel, P. Michaux, and M. Remoissenet, *Phys. Rev. E* **57**, 2320 (1998).
- [23] P. Tchofo Dinda, T. C. Kofane, and M. Remoissenet, *Phys. Rev. E* **60**, 7525 (1999).